A Wideband Leaky-Wave Lens Antenna with Annular Corrugations in the Ground Plane

Bosma, Sjoerd; Van Rooijen, Nick; Alonso-del Pino, Maria; Llombart , Nuria

DOI
10.1109/LAWP.2022.3176884

Publication date
2022

Document Version
Final published version

Published in
IEEE Antennas and Wireless Propagation Letters

A Wideband Leaky-Wave Lens Antenna With Annular Corrugations in the Ground Plane

Sjoerd Bosma, *Graduate Student Member, IEEE*, Nick van Rooijen, Maria Alonso-delPino, *Senior Member, IEEE*, and Nuria Llombart, *Fellow, IEEE*

***Abstract*—We present a resonant leaky-wave lens antenna, fed by a circular waveguide with annular corrugations in the ground plane. The proposed leaky-wave feed reduces the impact of the spurious TM_0 leaky-wave mode in all planes over a wide bandwidth while reducing assembly complexity compared to previous methods. The proposed leaky-wave antenna has an aperture efficiency above 80%, a return loss below −15 dB, and a cross-polarization level below −20 dB over a bandwidth from 110–220 GHz (2:1). We have fabricated and measured a WR-5 band (140–220 GHz) antenna prototype with a lens diameter of 3 cm that achieves excellent agreement between measurement and simulation in terms of return loss, directivity, and gain.**

***Index Terms*—Leaky-wave (LW) antenna, lens antenna, millimeter-wave, submillimeter-wave antennas, wideband antennas.**

I. Introduction

DIELECTRIC lens antennas fed by resonant leaky-wave (LW) feeds have been demonstrated at millimeter and submillimeter wavelengths, achieving high aperture efficiency and low losses [1]–[4] for communication and sensing applications. Due to their high directivity and aperture efficiency, they have been proposed as lens elements in scanning lens phased arrays [3], [4], and fly's eye arrays [2].

Resonant LW feeds consist of a half-wavelength resonant air cavity between a ground plane and a semi-infinite dielectric material with relative permittivity ε_r (i.e., the dielectric lens). This resonant Fabry–Pérot-like cavity supports the propagation of the main TM_1/TE_1 LW modes that contribute to generating a directive beam around broadside in the semi-infinite dielectric [1], [2], [5]. Additionally, a spurious, nearly frequency-independent TM_0 LW mode, which propagates in the cavity and results in high cross polarization, can reduce the aperture efficiency of the lens antenna. Therefore, the TM_0 mode is generally suppressed by the lens feed. Examples are a waveguide-fed double-slot iris [1], [2], a slot-fed dipole in PCB technology [3] and a dipole centered in the air cavity [6]. Although these LW feeds illuminate the lens with high aperture efficiency, the cross-polarization level of these antennas remains high when operated over a broad bandwidth due to poor TM_0 mode suppression. Furthermore, the development of double-slot irises is complex at (sub-)THz frequencies due to the need for a thin membrane [1], [2]. A recent overview of the state of the art in integrated lens antennas was given in [2].

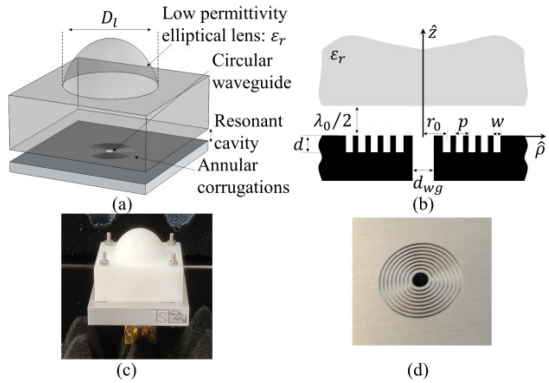

Fig. 1. (a) Geometry of the proposed LW lens antenna. (b) Dimensions of the feed stratification consisting of a circular waveguide, corrugated ground plane, air cavity, and semi-infinite medium. Photographs of (c) the assembled prototype and of (d) the circular waveguide and annular corrugations.

Metallic corrugations, by contrast, can be fabricated with the same process as the waveguide itself. It is well known that quarter-wavelength corrugations can be used in parallel-plate waveguides (PPW) to attenuate the TEM mode [7]–[9]. They are also used as mode filters in horn antennas [10]. Corrugated ground planes with waveguides have been used to generate a single LW mode around broadside [11], [12] with a nonrotationally symmetric beam and in shielded Fabry–Pérot cavity antennas to enhance the aperture efficiency [13]. However, those geometries have not explored the possibility of using the corrugations to reduce the impact of the TM_0 LW mode in resonant LW lens antennas.

In this letter, we propose a resonant LW lens antenna feed (see Fig. 1) that greatly reduces the impact of the TM_0 mode in all planes over a wide bandwidth. At high frequencies, the TM_0 is suppressed due to the electrical size of a circular waveguide. At low frequencies, annular corrugations in the ground plane increase the attenuation constant of the TM_0 LW mode, similar to a TEM PPW mode, enhancing the rotational symmetry and cross polarization of the feed pattern. We present the optimization of the proposed feed to illuminate a plastic lens with high aperture efficiency covering the WR-6 and WR-5 waveguide bands (110–220 GHz in total). The obtained performance is better than state-of-the-art plastic lens antennas [2] while reducing

Manuscript received 22 February 2022; revised 18 April 2022; accepted 5 May 2022. Date of publication 23 May 2022; date of current version 4 August 2022. This work was supported by the ERC Starting under Grant LAA-THz-CC 639749. *(Corresponding author: Sjoerd Bosma.)*

The authors are with the Terahertz Sensing Group, Delft University of Technology, 2628 CD Delft, The Netherlands (e-mail: s.bosma@tudelft.nl; n.van rooijen@tudelft.nl; m.alonsodelpino@tudelft.nl; n.llombartjuan@tudelft.nl).

Digital Object Identifier 10.1109/LAWP.2022.3176884

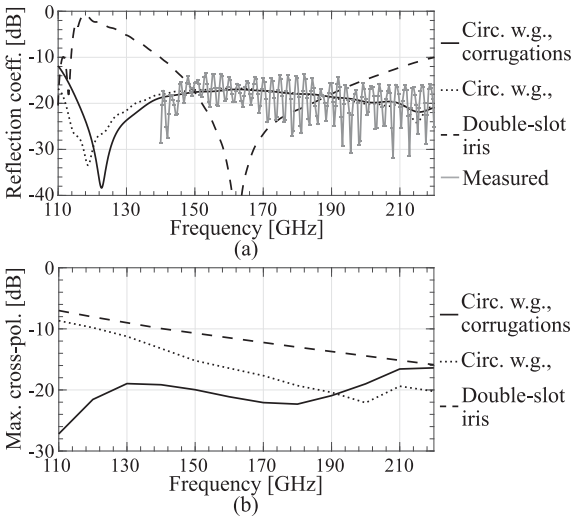

Fig. 2. (a) Simulated reflection coefficient and (b) cross polarization in the primary field of the three compared LW feeds: double-slot, circular waveguide, and corrugated circular waveguide. The measured S_{11} is shown in (a).

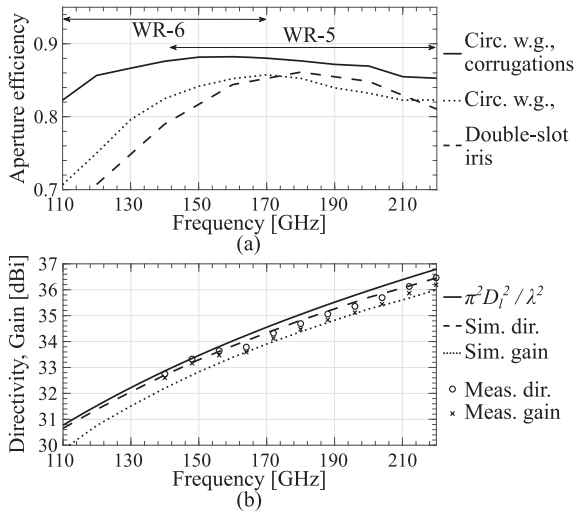

Fig. 3. (a) Simulated aperture efficiency for the same feeds as in Fig. 2 and (b) Simulated and measured directivity and gain of corrugated LW feed. The circles and crosses correspond to measured directivity and gain, respectively.

assembly complexity. We have manufactured and measured a WR-5 (140–220 GHz) prototype to corroborate these results.

II. Corrugated Leaky-Wave Antenna

The proposed LW lens antenna geometry is shown in Fig. 1(a) and (b). It consists of a $\lambda_0/2$ air cavity with a low-permittivity ($\varepsilon_r = 2.3$) elliptical dielectric lens to achieve wide bandwidth, as in [2]. The feeding structure is modified with respect to [2]. An open-ended circular waveguide, without a double-slot iris, is proposed here in combination with annular corrugations in the ground plane surrounding the waveguide. The low air–dielectric contrast ensures good impedance matching of the waveguide over a wide bandwidth. A large circular waveguide can achieve better suppression of the TM_0 LW mode in all azimuthal directions compared to a square waveguide. However, a large diameter of such circular waveguide will lead to a significant frequency variation of the primary field (i.e., field radiated into the semi-infinite dielectric medium). Consequently, poor lens aperture efficiency over a large bandwidth will be achieved. Therefore, we have added annular corrugations in the ground plane that reduce the impact of the TM_0 LW mode close to the cut-off frequency of the waveguide, and therefore enlarge the antenna's overall bandwidth.

A. Geometry Optimization for 2:1 Bandwidth

The proposed LW feed geometry has been optimized for its operation in a 2:1 bandwidth (110–220 GHz). First, the circular waveguide diameter is chosen to be the smallest possible to achieve a good impedance match starting at 110 GHz while exciting only the fundamental mode. A diameter $d_{wg} = 0.95\,\lambda_0$ leads to a cut-off frequency of 102 GHz giving a good compromise between the excitation of higher order modes at high frequencies and the impedance match at low frequencies. The achieved reflection coefficient (S_{11}) is below -15 dB over the entire bandwidth of interest, see Fig. 2(a). For reference, the achieved impedance matching bandwidth with a double-slot iris feed as in [2] is also given. The achieved cross polarization of this feed is shown in Fig. 2(b).

Second, we maximize the aperture efficiency of a truncated elliptical dielectric lens with a diameter of 3 cm ($16.5\,\lambda_0$, λ_0 being defined at 165 GHz) over the entire 110–220 GHz bandwidth to find the optimal corrugation dimensions. The performance of this lens antenna is evaluated using the analysis procedure described in [2]: First, the primary fields are obtained in the entire bandwidth by a full-wave simulation for a specific feed structure. Second, the aperture efficiency of the lens is calculated in reception using the Fourier optics (FO) approach [14], optimizing for the phase center Δz and truncation angle θ_0 seen from the phase center, as defined in [2]. This procedure is iterated as a function of the depth (d), width (w), periodicity (p), and distance from the waveguide (r_0) of the corrugations as indicated in Fig. 1(b).

Starting from the dimensions in [8]: $d = p = \lambda_0/4$, $w = \lambda_0/10$, we found the optimized dimensions to be $d = 0.33\,\lambda_0$, $p = 0.23\,\lambda_0$, $w = 0.11\,\lambda_0$, $r_0 = 0.69\,\lambda_0$. We found that geometries with 8 corrugations are sufficient to enhance the aperture efficiency at the low frequencies. The phase center and truncation angle that maximize the aperture efficiency are found as $\Delta z = -0.66\,\lambda_0$ and $\theta_0 = 36.5°$, respectively. The optimized phase center and lens truncation angle are in line with the theoretical ones in [15] based on the LW propagation constants of the TM_1 and TE_1 modes.

The aperture efficiency as a function of the frequency for the optimized lens antenna with a corrugated LW feed is shown in Fig. 3(a). The aperture efficiency is above 80% over the entire bandwidth, which is significantly higher than the same antenna without corrugations and the double-slot iris feed, especially at the low frequencies. The figure indicates that the circular waveguide feed without corrugations performs similar to the double-slot iris in the WR-5 band (with a significant reduction in the fabrication assembly). If an extended bandwidth is targeted (WR-5 and WR-6), the corrugated LW feed is the best performing solution. The achieved reflection coefficient with this

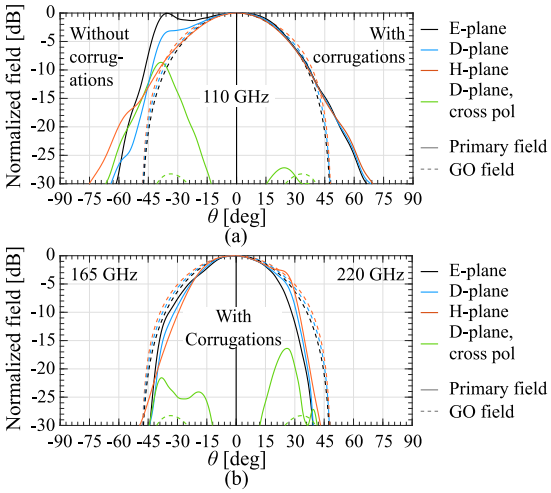

Fig. 4. Comparison between the primary and GO fields. (a) Fields at 110 GHz of the LW feed without (left) or with (right) corrugations. (b) Fields of the LW feed with corrugations at 165 GHz (left) and 220 GHz (right).

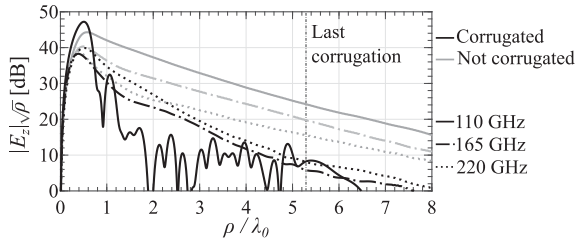

Fig. 5. Electric field along $\hat{z}$ at $z = h/2$ as a function of the radial direction in the D-plane for the LW feed with or without corrugations at three frequencies.

corrugated feed is in line with the one without the corrugations as shown in Fig. 2(a).

B. Radiation Patterns in the Semi-Infinite Dielectric Medium

To better understand the enhancement of the aperture efficiency achieved due to the corrugations, it is useful to compare the primary fields at 110 GHz with or without corrugations as shown in Fig. 4(a). The primary patterns of the corrugated waveguide are significantly more rotationally symmetric and have lower cross polarization. The cross-polarization level is reduced from -8 dB to -27 dB when the corrugations are added. The cross polarization in the primary fields over the entire bandwidth is reported in Fig. 2(b) for the three considered LW feeds. At the high end of the bandwidth, the cross polarization of the circular waveguide with and without corrugations is comparable. Indeed, the suppression of the TM_0 LW mode is achieved at the higher part of the band thanks to the large size of the circular waveguide and not the corrugations.

The aperture efficiency can be calculated as a field match between the field on a sphere centered at the lens focus propagated via geometrical optics (GO) from an incident plane wave on the lens, i.e., the GO field, and the feed primary pattern [14]. The highest aperture efficiency is achieved when these fields are a conjugate match. The frequency-independent GO field was given in [2] and is also shown in Fig. 4 (dashed lines) for comparison. It is clear from Fig. 4(a) that the field match to the GO field is much better at the low-frequency band if the corrugations are used. The primary patterns of the corrugated LW feed at 165 GHz and 220 GHz are shown in Fig. 4(b). A good match between the incident GO field and the primary patterns is observed leading to aperture efficiency higher than 80% over the entire bandwidth.

C. TM_0 Mode Suppression

To understand the effect that the corrugations have on the TM_0 LW poles, we analyzed the fields in the resonant cavity using full-wave simulations with a large number of corrugations, i.e., 20. Radially close to the waveguide [$\rho \leq \lambda_0$, see Fig. 1(b)], the field is given by the sum of the space wave contribution and the TM_1/TE_1 LW modal fields [15]. For larger ρ, the TM_0 modal field is dominant. Since the TM_0 modal field is mostly polarized along $\hat{z}$ [4], we can study the effect of the corrugations by analyzing the $\hat{z}$-component of the electric field in the middle of the resonant cavity (i.e., at $z = h/2$) as a function of ρ. We show $|E_z|\sqrt{\rho}$ in the D-plane in Fig. 5 to remove the cylindrical spreading of the LW modal fields. The figure compares the LW feed with and without the corrugations at the beginning, middle, and end of the bandwidth. The results show that the $|E_z|\sqrt{\rho}$ level at the end of the corrugated section is lower when the corrugations are present. The highest attenuation is achieved at low frequencies.

It is well known that periodic structures do not fully suppress a mode, but do impact its attenuation constant [9]. Since the modal field is proportional to $e^{-j\beta_{TM0}\rho}e^{-\alpha_{TM0}\rho}/\sqrt{\rho}$ [9], the TM_0 phase, β_{TM0}, and attenuation, α_{TM0}, constants can be calculated from the simulated E_z. At the central frequency and with no corrugations, it is found that $\beta_{TM0}/k_d = 0.6$ and $\alpha_{TM0}/k_d = 0.045$, in line with the analytical result from the dispersion equation [2]. The attenuation constant corresponds to -3.7 dB/λ_0. For the corrugated ground plane, $\alpha_{TM0}/k_d = 0.086$ has been found, which corresponds to -7.1 dB/λ_0. Therefore, the corrugations decrease the impact of the TM_0 mode even in the middle of the bandwidth.

D. Lens Antenna Radiation Performance

We calculated the radiation patterns of the lens antenna fed by the proposed corrugated LW feed (secondary patterns) using the FO approach in reception [14]. The secondary patterns are shown in Fig. 6(a) and (b) at 140 and 220 GHz, respectively. The patterns are highly symmetric around broadside and achieve a sidelobe level of between -20 to -17 dB in the bandwidth, which is very close to the sidelobe level of a uniform circular current distribution of 3 cm in diameter. The simulated cross polarization of the secondary patterns is below -25 dB across the full bandwidth.

The simulated directivity and gain of the lens antenna are shown in Fig. 3(b) as a function of the frequency. The directivity and gain have been calculated using full-wave simulations of the lens antenna in CST. For the gain, the dielectric losses in the plastic (below 0.5 dB) and ohmic losses in the aluminum ground plane (below 0.05 dB) are taken into account. The maximum directivity that can be achieved by a 3 cm diameter lens is shown for reference, which is at most 0.2 dB higher than the

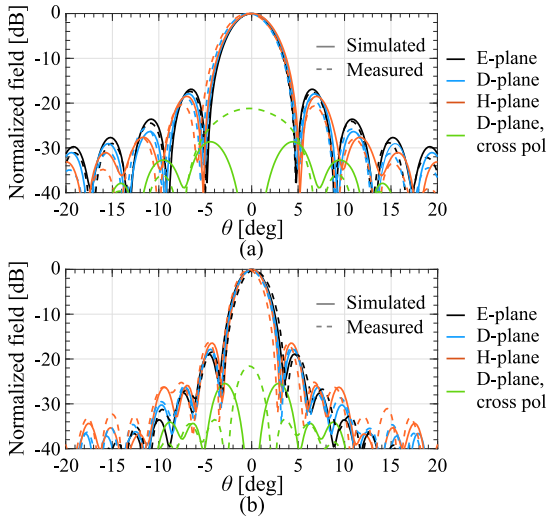

Fig. 6. Simulated (solid) and measured (dashed) radiation patterns at (a) 140 and (b) 220 GHz.

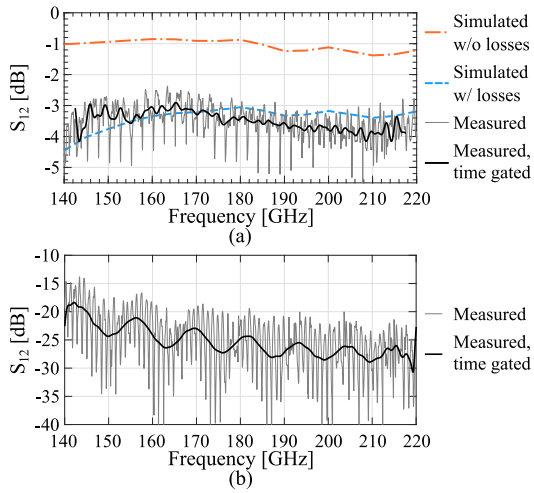

Fig. 7. Simulated and measured near-field coupling between two lenses that are (a) co- and (b) cross-polarized.

simulated directivity. The simulated gain is around 0.8 dB below the maximum achievable directivity in the full bandwidth.

III. Validation With WR-5 Antenna Prototype

We have fabricated and measured two identical G-band (WR-5, 140–220 GHz) prototypes to validate the simulated performance. The fabricated antennas, shown in Fig. 1(c), consist of an HDPE lens with a diameter of 3 cm and a 1 cm thick aluminum split block with a WR-5 flange on the bottom that is tapered to a circular waveguide. A CNC milling process was used for the fabrication of the lens and the split block; the corrugations were milled into the ground plane after assembling the split block, see Fig. 1(d).

The measured reflection coefficient of the antenna prototype is shown in Fig. 2(a). An excellent agreement is achieved with the simulated value: below -15 dB in the entire bandwidth. The antenna prototype was measured on a planar near-field antenna measurement setup using a PNA with WR-5 frequency extenders. A WR-5 waveguide probe was used to sample the field at 4 cm above the lens surface. The far-field radiation patterns were calculated from the two-dimensional near-field scans using standard near-to-far field conversion. The obtained radiation patterns are shown in Fig. 6(a) and (b) at 140 and 220 GHz with excellent agreement to full-wave simulations. The increase in measured cross polarization is due to limited fabrication tolerances in the waveguide split-block transition which causes the excitation of the orthogonal mode in the circular waveguide. As a result, the measured cross-polarized patterns have a similar shape to the co-polarized patterns. The measured directivity is compared to the simulated values in Fig. 3(b), giving a very good agreement between measurement and simulation in the entire WR-5 band. The machining tolerance achieved in corrugations was less than 20 μm and was found not to have a significant effect on the performance.

The procedure in [2] has been followed to measure the gain. Two lenses were placed facing each other at a distance of 1.5 cm, and the S_{12} was measured. The result is shown in Fig. 7(a) in gray. The raw measurements oscillate ± 1 dB around the time-gated value (black), a significant improvement with respect to the 8 dB in [2], which we attribute to the higher aperture efficiency achieved. For comparison to the simulations, the S_{12} has been time-gated after the first received pulse as in [2]. The simulation results in a lens-to-lens coupling of around -1 dB in the entire WR-5 band, i.e., around 90% efficiency per lens. The losses in the waveguide are lower than 1.6 dB ($\sigma = 3.6 \cdot 10^5$ S/m) and the losses in the plastic lens are below 0.3 dB ($\tan\delta = 3.3 \cdot 10^{-4}$). When the losses are combined with the semi-analytical simulation, the lens-to-lens coupling is around -3.5 dB, which is in excellent agreement with the measured value. The measured antenna gain, shown in Fig. 3(b), is calculated from the measured directivity and takes into account the dielectric loss in the lens. The gain is in excellent agreement with simulations.

The cross-polarization broadside level was measured using the same procedure, but with one antenna rotated 90° around ϕ. The simulated coupling between orthogonal antennas is zero owing to the null at broadside in the simulated cross-polarized pattern. However, due to the limited fabrication accuracy in the waveguide split block, the measured coupling is between -20 and -30 dB as shown in Fig. 7(b), which is in line with the measured cross-polarization level at broadside (Fig. 6).

V. Conclusion

We have presented a resonant leaky-wave antenna feed for plastic lenses that includes annular corrugations in the ground plane around a circular waveguide. These corrugations in combination with the circular waveguide significantly reduce the impact of the spurious TM_0 mode in a wide bandwidth and all azimuthal planes. The corrugations extend the achieved bandwidth of the circular waveguide feed to lower frequencies to cover both the WR-5 and WR-6 bands, leading to a total bandwidth of 2:1. A lens illuminated by such LW feed is shown to have cross-polarization level below -20 dB, an aperture efficiency above 80% and an S_{11} below -15 dB over the entire bandwidth. We fabricated and measured a WR-5 band prototype which shows excellent agreement with the anticipated results.

REFERENCES

[1] N. Llombart, G. Chattopadhyay, A. Skalare, and I. Mehdi, "Novel terahertz antenna based on a silicon lens fed by a leaky wave enhanced waveguide," *IEEE Trans. Antennas Propag.*, vol. 59, no. 6, pp. 2160–2168, Jun. 2011, doi: 10.1109/TAP.2011.2143663.

[2] M. Arias Campo, D. Blanco, S. Bruni, A. Neto, and N. Llombart, "On the use of fly's eye lenses with leaky-wave feeds for wideband communications," *IEEE Trans. Antennas Propag.*, vol. 68, no. 4, pp. 2480–2493, Apr. 2020, doi: 10.1109/TAP.2019.2952474.

[3] H. Zhang, S. Bosma, A. Neto, and N. Llombart, "A dual-polarized 27-dBi scanning lens phased array antenna for 5G point-to-point communications," *IEEE Trans. Antennas Propag.*, vol. 69, no. 9, pp. 5640–5652, Sep. 2021, doi: 10.1109/TAP.2021.3069494.

[4] M. Alonso-delPino, S. Bosma, C. Jung-Kubiak, G. Chattopadhyay, and N. Llombart, "Wideband multimode leaky-wave feed for scanning lens-phased array at submillimeter wavelengths," *IEEE Trans. Terahertz Sci. Technol.*, vol. 11, no. 2, pp. 205–217, Mar. 2021, doi: 10.1109/TTHZ.2020.3038033.

[5] D. R. Jackson and A. A. Oliner, "A leaky-wave analysis of the high-gain printed antenna configuration," *IEEE Trans. Antennas Propag.*, vol. 36, no. 7, pp. 905–910, Jul. 1988, doi: 10.1109/8.7194.

[6] M. Arias Campo *et al.*, "H-band quartz-silicon leaky-wave lens with air-bridge interconnect to GaAs front-end," *IEEE Trans. Terahertz Sci. Technol.*, vol. 11, no. 3, pp. 297–309, May 2021, doi: 10.1109/TTHZ.2021.3049640.

[7] P. S. Kildal, "Artificially soft and hard surfaces in electromagnetics," *IEEE Trans. Antennas Propag.*, vol. 38, no. 10, pp. 1537–1544, Oct. 1990, doi: 10.1109/8.59765.

[8] P. S. Kildal, E. Alfonso, A. Valero-Nogueira, and E. Rajo-Iglesias, "Local metamaterial-based waveguides in gaps between parallel metal plates," *IEEE Antennas Wireless Propag. Lett.*, vol. 8, pp. 84–87, 2009.

[9] N. Llombart, A. Neto, G. Gerini, and P. de Maagt, "Planar circularly symmetric EBG structures for reducing surface waves in printed antennas," *IEEE Trans. Antennas Propag.*, vol. 53, no. 10, pp. 3210–3218, Oct. 2005, doi: 10.1109/TAP.2005.856365.

[10] B. Thomas, "Design of corrugated conical horns," *IEEE Trans. Antennas Propag.*, vol. AP-26, no. 2, pp. 367–372, Mar. 1978, doi: 10.1109/TAP.1978.1141842.

[11] M. Beruete *et al.*, "Very low-profile 'bull's eye' feeder antenna," *IEEE Antennas Wireless Propag. Lett.*, vol. 4, pp. 365–368, 2005, doi: 10.1109/LAWP.2005.851104.

[12] A. Sutinjo and M. Okoniewski, "A simple leaky-wave analysis of 1-D grooved metal structure for enhanced microwave radiation," *IEEE Trans. Antennas Propag.*, vol. 60, no. 6, pp. 2719–2726, Jun. 2012, doi: 10.1109/TAP.2012.2194655.

[13] S. A. Muhammad, R. Sauleau, and H. Legay, "Small-size shielded metallic stacked Fabry–Perot cavity antennas with large bandwidth for space applications," *IEEE Trans. Antennas Propag.*, vol. 60, no. 2, pp. 792–802, Feb. 2012, doi: 10.1109/TAP.2011.2173133.

[14] H. Zhang, S. O. Dabironezare, G. Carluccio, A. Neto, and N. Llombart, "A fourier optics tool to derive the plane wave spectrum of quasi-optical systems," *IEEE Antennas Propag. Mag.*, vol. 63, no. 1, pp. 103–116, Feb. 2021, doi: 10.1109/MAP.2020.3027233.

[15] S. Bosma, A. Neto, and N. Llombart, "On the near-field spherical wave formation in resonant leaky-wave antennas: Application to small lens design," *IEEE Trans. Antennas Propag.*, vol. 70, no. 2, pp. 801–812, Feb. 2022, doi: 10.1109/TAP.2021.3137238.